Journal of Physics: Conference Series

Theoretical Derivation of Gauges for Straddle-type Monorail Vehicle

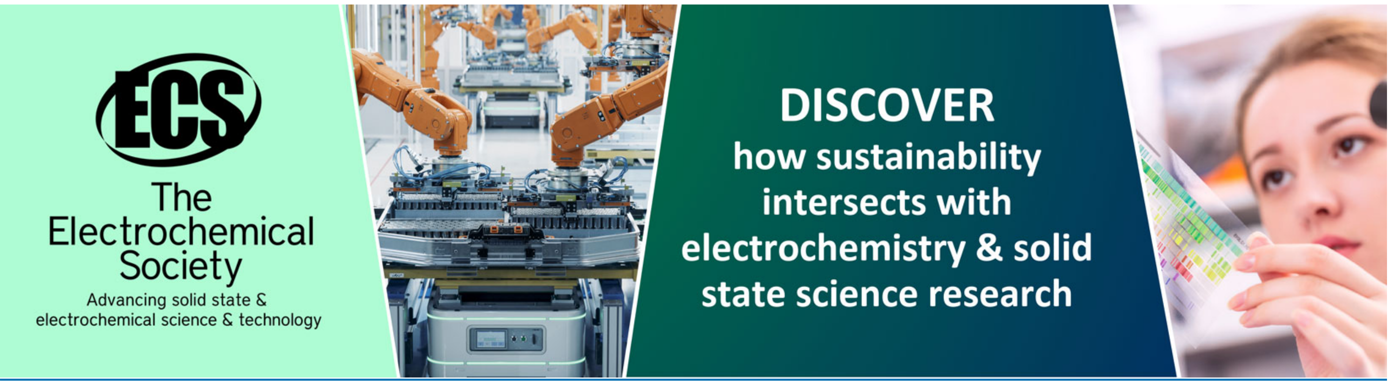

Theoretical Derivation of Gauges for Straddle-type Monorail Vehicle

Jiancai Zou*, Bingyan Chen, Shen Zhan, Chao Huang and Xiaojun Wang

CRRC Qingdao Sifang Co., Ltd, Qingdao, China
Email: zoujiancai@cqsf.com

Abstract. The theoretical model of the straddle-type monorail vehicle bogie is set up and the function of each component is introduced. The lateral and vertical displacements of carbody when the lateral and roll motion of carbody in the same/reverse direction are attained through theoretical derivation, which can be put into the calculation of the vehicle gauge. A computational program is written to simulate the corresponding results under specific parameters. The correctness of the method to calculate the monorail vehicle gauge is verified.
Keywords. Straddle-type monorail vehicle, Gauge, Formula derivation.

1. Introduction

With the booming economic development and the acceleration of the urbanization, it is absolutely important to improve the transportation system, especially in the railway transit [1]. As a brand-new type of urban rail transit vehicle, the transportation volume of straddle-type monorail vehicle is moderate, with a small covering area and a strong terrain adaptability, which has wide application prospects [2]. Therefore, numerous studies have been conducted by researchers to explore the dynamic performances of straddle-type monorail vehicles.

Zhang et al. studied the anti-overturning stability of a typical straddle-type monorail vehicle, they derived a formula to describe the relationship between critical lateral force and the pre-load of the stabilizing wheels from the lateral roll equation, which was verified through UM software [3-4]. Zhu et al. put up with an idea that the adjustment of width of monorail beams can polish the dynamic performances of monorail train, through which they attained the deformation equations of the steering wheels and stabilizing wheels in terms of contact relationship, proving that a proper width of monorail beam can greatly decrease the tire deformation on curved track [5]. Jiang et al. established two types of articulated monorail vehicle models. By utilizing genetic algorithm, they compared the dynamic properties between them, reaching a conclusion that the non-bolster type of monorail vehicle is advantageous in passing the radius curve [6-7]. Bao et al. carried out studies concerned with the dynamic response and safety analysis of a monorail vehicle through ANSYS and SIMPACK, proposing that the vibration of the vehicle should be reduced and the track irregularity is negative to the system [8].

Obviously, the dynamic performances of monorail vehicles have been studied deeply by researchers, however, the calculation method of vehicle gauge is still nonstandard, and there is no clearer method for the gauge of straddle monorail vehicles in China. Therefore, this paper combined theoretical derivation with computational simulation to calculate the gauge for monorail vehicles. Firstly, the theoretical model of the monorail vehicle was introduced, with the main structures presented. Then, the lateral and vertical displacements of the carbody under different working conditions were derived based on Ref [9-10]. Finally, a program was written to calculate the corresponding parameters, and the gauge result was acquired, which verified the calculation formulas.

2. Theoretical Model

Figure 1 presents a typical straddle-type monorail vehicle that is running on the track in Chongqing city, whose configuration is made up of carbody, bogie and track system.

Figure 1. Straddle-type monorail vehicle.

Figure 2 illustrates a representative structure of straddle-type monorail vehicle bogie, which consists of frame, air spring, traction motor, center pivot, collector and four types of rubber wheels. When vehicle is running on tracks, the running wheel will always be in contact with the top surface of the track beam, decreasing the vertical vibration, while the stabilizing wheel and the guiding wheel can reduce the lateral vibration. In addition, the auxiliary wheel can be utilized as running wheel if the air leakage happens.

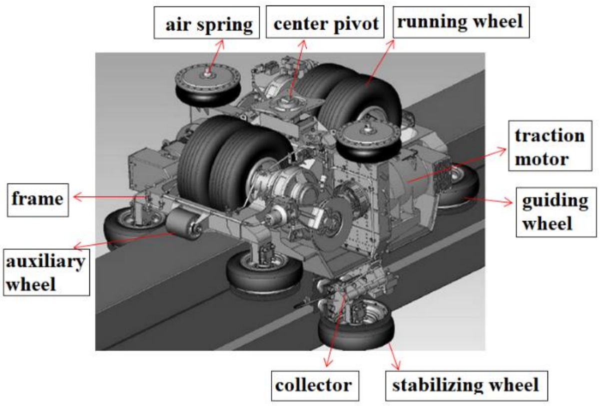

Figure 2. Structure of straddle-type monorail vehicle bogie.

Since the movement posture of straddle-type monorail vehicles is similar to that of traditional railway vehicles, the calculation formula of dynamic gauges can refer to relevant standards [9-10]. However, as the straddle-type monorail does not use the steel wheel/rail structure, but uses rubber wheels, there is a distinct difference in the calculation of the wheel/rail relationship and parameters.

3. Derivation of Calculation Formula

3.1. Lateral and Roll Displacement of Carbody in the Same Direction

When the monorail vehicle runs on the track, the carbody will have offsets mainly in the lateral and vertical direction due to the corresponding forces, which should be considered in the calculation of vehicle gauges. If the lateral displacement and the roll motion of carbody are in the same direction, then the lateral displacement of carbody can be expressed as equation (1).

$$\Delta X_{BP}=\left(\Delta X_{dw}+\Delta w_0+\Delta w_2+\Delta q_1\right)\frac{2n+a}{a}+\Delta_e+\Delta\theta_{t2}\cdot Y\cdot\left(1+S\right)+100m_z g\left(1+S\right)\left(\frac{Y-h_{cp}}{K_{\varnothing p}}+\frac{Y-h_{cs}}{K_{\varnothing s}}\right)+\sqrt{\begin{array}{c}\Delta M_{Bx}{}^2+\Delta C^2+\left[\Delta\theta_{t1}\cdot Y\cdot\left(1+S\right)\right]^2+\left[A_w\cdot P_w\cdot\left(1+S\right)C_h\right]^2+\left[m_B\cdot a_B\left(1+S\right)C_h^{'}\right]^2\\+\Delta M_{t1}{}^2+\Delta M_{t2}{}^2+\left[\frac{\Delta X_{Bq}}{H_{cq}}\left(Y-H_{sj}\right)\right]^2+\left(\Delta w_1\cdot\frac{2n+a}{a}\right)^2+\left(\frac{\Delta d}{2}\cdot\frac{2n+a}{a}\right)^2\end{array}} \tag{1}$$

where

$$C_h=\left(\mathrm{Y}-h_{cp}\right)\cdot\frac{h_{sw}-h_{cp}}{K_{\varnothing p}}+\left(Y-h_{cs}\right)\cdot\frac{h_{sw}-h_{cs}}{K_{\varnothing s}} \tag{2}$$

$$C_h=\left(\mathrm{Y}-h_{cp}\right)\cdot\frac{h_{sc}-h_{cp}}{K_{\varnothing p}}+\left(Y-h_{cs}\right)\cdot\frac{h_{sc}-h_{cs}}{K_{\varnothing s}} \tag{3}$$

$$\mathrm{S}=m_B g\left[\frac{h_{sc}-h_{cp}}{K_{\varnothing p}}+\frac{h_{sc}-h_{cs}}{K_{\varnothing s}}\right] \tag{4}$$

$$K_{\varnothing s}=0.5n_s c_s b_s{}^2 \tag{5}$$

For the vertical upward displacement of carbody,

$$\Delta Y_{BPU}=f_2+\Delta M_{qc\_up}+\sqrt{\Delta M_{t3}{}^2+\Delta M_{By}{}^2+\left(\Delta f_p\cdot\frac{2n+a}{a}\right)^2+\left(\Delta f_s\cdot\frac{2n+a}{a}\right)^2+\sigma_c{}^2}-\left[\begin{array}{c}\Delta\theta_{t2}\left(1+S\right)X+100m_z g\left(1+S\right)X\left(\frac{1}{K_{\varnothing p}}+\frac{1}{K_{\varnothing s}}\right)+\\\sqrt{\begin{array}{c}\left[\Delta\theta_{t1}\cdot X\left(1+S\right)\right]^2+\left[A_w\cdot P_w\left(1+S\right)X\left(\frac{h_{sw}-h_{cp}}{K_{\varnothing p}}+\frac{h_{sw}-h_{cs}}{K_{\varnothing s}}\right)\right]^2\\+\left[m_B\cdot a_B\left(1+S\right)X\left(\frac{h_{sc}-h_{cp}}{K_{\varnothing p}}+\frac{h_{sc}-h_{cs}}{K_{\varnothing s}}\right)\right]^2+\left(\frac{\Delta X_{Bq}}{H_{cq}}\cdot X\right)^2\end{array}}\end{array}\right] \tag{6}$$

For the vertical downward displacement of carbody,

$$\Delta Y_{BPd}=f_{01}+f_1+f_2+f_{02}+\sigma_e+\sigma_w+\Delta M_{qc_{-down}}+\Delta\theta_{t2}\left(1+S\right)X+100m_z g\left(1+S\right)X\left(\frac{1}{K_{\varnothing p}}+\frac{1}{K_{\varnothing s}}\right)+\sqrt{\begin{array}{c}\Delta M_{By}{}^2+\delta_c{}^2+\Delta M_{t4}{}^2+\left(\Delta f_p\cdot\frac{2n+a}{a}\right)^2+\left(\Delta f_s\cdot\frac{2n+a}{a}\right)^2\\+\left[\Delta\theta_{t1}\cdot X\left(1+S\right)\right]^2+\left(\frac{\Delta X_{Bq}}{H_{cq}}\cdot X\right)^2+\left[A_w\cdot P_w\left(1+S\right)X\left(\frac{h_{sw}-h_{cp}}{K_{\varnothing p}}+\frac{h_{sw}-h_{cs}}{K_{\varnothing s}}\right)\right]^2\\+\left[m_B\cdot a_B\left(1+S\right)X\left(\frac{h_{sc}-h_{cp}}{K_{\varnothing p}}+\frac{h_{sc}-h_{cs}}{K_{\varnothing s}}\right)\right]^2\end{array}} \tag{7}$$

3.2. Lateral and Roll Displacement of Carbody in the Reverse Direction

Similar to section 3.1, when the lateral displacement and the roll motion of carbody are in the reverse direction, then the lateral displacement of carbody can be expressed as equation (8).

$$\begin{aligned}\Delta X_{BP} &= \left(\Delta X_{dw}+\Delta w_0+\Delta w_2+\Delta q_1\right)\frac{2n+a}{a}+\Delta_e \\ &+\sqrt{\Delta M_{Bx}{}^2+\Delta C^2+\Delta M_{t1}{}^2+\Delta M_{t2}{}^2+\left(\Delta w_1\cdot\frac{2n+a}{a}\right)^2+\left(\frac{\Delta d}{2}\cdot\frac{2n+a}{a}\right)^2} \\ &-\left[\begin{gathered}\Delta\theta_{t2}\cdot Y\cdot(1+S)+100m_z g(1+S)\left(\frac{Y-h_{cp}}{K_{\varnothing p}}+\frac{Y-h_{cs}}{K_{\varnothing s}}\right)+ \\ \sqrt{\begin{gathered}\left[\Delta\theta_{t1}\cdot Y\cdot(1+S)\right]^2+\left[A_w\cdot P_w\cdot(1+S)C_h\right]^2+\left[m_B\cdot a_B(1+S)C_h'\right]^2 \\ +\left[\frac{\Delta X_{Bq}}{H_{cq}}\left(Y-H_{sj}\right)\right]^2\end{gathered}}\end{gathered}\right]\end{aligned} \tag{8}$$

For the vertical upward displacement of carbody,

$$\begin{aligned}\Delta Y_{BPU} &= f_2+\Delta M_{qc\_up}+\Delta\theta_{t2}(1+S)X+100m_z g(1+S)X\left(\frac{1}{K_{\varnothing p}}+\frac{1}{K_{\varnothing s}}\right)+ \\ &\sqrt{\begin{gathered}\Delta M_{t3}{}^2+\Delta M_{By}{}^2+\sigma_c{}^2+\left(\Delta f_p\cdot\frac{2n+a}{a}\right)^2+\left(\Delta f_s\cdot\frac{2n+a}{a}\right)^2 \\ +\left[\Delta\theta_{t1}\cdot X(1+S)\right]^2+\left(\frac{\Delta X_{\mathrm{Bq}}}{H_{cq}}\cdot X\right)^2+\left[A_w\cdot P_w(1+S)X\left(\frac{h_{sw}-h_{cp}}{K_{\varnothing p}}+\frac{h_{sw}-h_{cs}}{K_{\varnothing s}}\right)\right]^2 \\ +\left[m_B\cdot a_B(1+S)X\left(\frac{h_{sc}-h_{cp}}{K_{\varnothing p}}+\frac{h_{sc}-h_{cs}}{K_{\varnothing s}}\right)\right]^2\end{gathered}}\end{aligned} \tag{9}$$

For the vertical downward displacement of carbody,

$$\Delta Y_{BPd} = f_{01} + f_1 + f_2 + f_{02} + \sigma_e + \sigma_w + \Delta M_{qc_{-\text{down}}} + \sqrt{\Delta M_{By}{}^2 + \delta_c{}^2 + \Delta M_{t4}{}^2 + \left(\Delta f_p \cdot \frac{2n+a}{a}\right)^2 + \left(\Delta f_s \cdot \frac{2n+a}{a}\right)^2} - \left[\begin{array}{c} \Delta\theta_{t2}\left(1+S\right)X + 100 m_z g\left(1+S\right)X\left(\frac{1}{K_{\varnothing p}} + \frac{1}{K_{\varnothing s}}\right) + \\ \sqrt{\begin{array}{c}\left[\Delta\theta_{t1}\cdot X\left(1+S\right)\right]^2 + \left[A_w \cdot P_w\left(1+S\right)X\left(\frac{h_{sw}-h_{cp}}{K_{\varnothing p}} + \frac{h_{sw}-h_{cs}}{K_{\varnothing s}}\right)\right]^2 + \\ \left[m_B \cdot a_B\left(1+S\right)X\left(\frac{h_{sc}-h_{cp}}{K_{\varnothing p}} + \frac{h_{sc}-h_{cs}}{K_{\varnothing s}}\right)\right]^2 + \left(\frac{\Delta X_{\mathrm{Bq}}}{H_{cq}}\cdot X\right)^2\end{array}}\end{array}\right] \tag{10}$$

4. Simulation

As the calculation formulas of the carbody displacement are demonstrated in equation (1)-(10), a computational program is written to calculate the corresponding displacements in order to verify the derivation process, and part of the parameters used in the paper are shown in table 1.

Table 1. Vehicle parameters.

Parameters	**Values**
Length between bogie centers	a=7000 mm
Wheelbase between guiding wheel	p=1700 mm
Weight of carbody	m_b=23110 kg
Lateral manufacturing tolerance of guiding wheel	Δd=2 mm
Static lateral displacement between frame and track	ΔX_{dw}=2 mm
Vertical elastic deformations of running wheel	f_{01}=0 mm
Deflection of running wheel	f_1=15 mm
Installation tolerance between the secondary suspension	f_{02}=2 mm
Deflection of the secondary suspension	f_2=3 mm
Dynamic deflection of running wheel	Δf_p=5 mm
Lateral deformation of the secondary spring(static)	Δw_0=10 mm
Lateral deformation of the secondary spring(dynamic)	Δw_1=10 mm
Wears of center pivot	Δw=1 mm
Installation tolerance of center pivot	Δm_{t2}=1 mm
Dynamic deflection of secondary suspension upward	Δf_{ss}=20 mm
Distance between the secondary spring and rail	h_{cs}=-35.5 mm
Vertical stiffness of individual secondary spring	C_s=210 N/mm
Distance between the secondary spring	b_s=2170 mm
Height of side wall of carbody	h_{cq}=4616 mm
Area of wind area of carbody	a_w=54.6 m^2
Pressure of crosswind	p_w=500 N/m^2
Distance between the gravity center of carbody and rail	h_{sc}=1416 mm
Distance between the center of wind area and rail	h_{sw}=870 mm
Distance between bottom of carbody and rail	h_{sj}=537 mm
Gradient of the carbody	Δx_{bq}=10 mm
Lateral acceleration	a_b=0.5 m/s^2
Installation tolerance of the carbody surface devices	Δm_{t1}=2 mm
Installation tolerance of the carbody upward	Δm_{t3}=10 mm
Installation tolerance of the carbody downward	Δm_{t4}=2 mm

Parameters	Values
Tolerance of the floor	Δm_{t5}=5 mm
Lateral tolerance of track beam centerline	Δ_c=25 mm
Vertical tolerance of track beam centerline	σ_c=30 mm
Lateral deformation of track beam	Δ_e=3 mm
Vertical deformation of track beam	σ_e=15 mm
Inclination of track beam tolerance	$\Delta\theta_{t1}$=0.002 rad
Elastic inclination of track beam	$\Delta\theta_{t1}$=0.001 rad

Figure 3 illustrates a gauge calculation result when the straddle-type monorail vehicle is running on straight track. The construction gauge and the vehicle gauge are the standard of Ref [9], while the same gauge and the reverse gauge correspond to lateral and roll displacement of carbody in the same/reverse direction respectively. It is clear through figure 2 that both the same gauge and reverse gauge results can meet the requirement of the corresponding standards, which verifies the correctness of the calculation formulas.

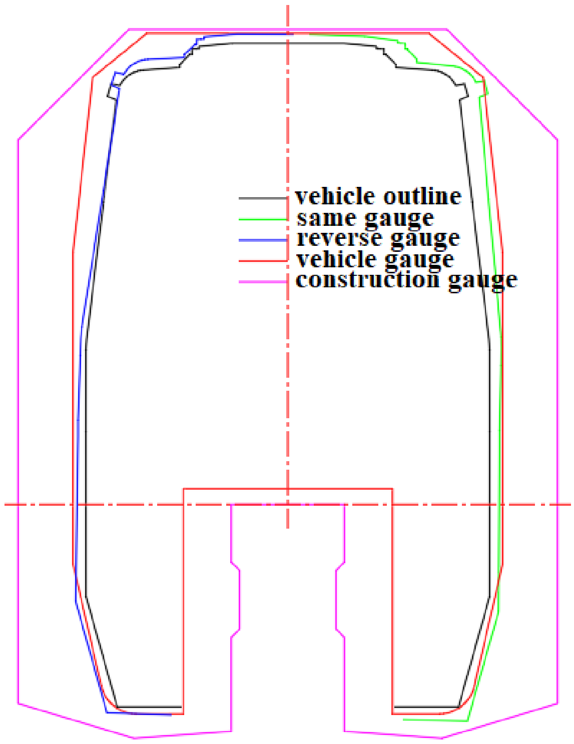

Figure 3. Gauge calculation result on straight track.

5. Conclusion

Based on the existing calculation method and theoretical model of monorail vehicle, the derivation of the carbody displacement under different working conditions was conducted. The calculation result was attained through a computational program under specific parameters, which satisfied the requirements of the standard and shall be a reference in calculating the gauge of monorail vehicles.

6. Acknowledgments

This work was supported by the National Key R&D Program (Grant No. 2018YFE0201400).

References

[1] Zhou J C, Du Z X and Yang Z 2020 Dynamic parameters optimization of straddle-type monorail vehicles based multi-objective collaborative optimization algorithm *Vehicle System Dynamics* **58** (3) 357-376

[2] Wang G L, Li K Q and Zhou H C 2019 Abnormal wear analysis of straddle-type monorail vehicle running wheel tire *Advances in Mechanical Engineering* **11** (11) 1-16

[3] Zhang R, Ji Y J and Ren L H 2019 Pre-load on the guiding/stabilizing wheels and the critical lateral force of a straddle-type monorail vehicle *Proceedings of the Institution of Mechanical Engineers, Part F: Journal of Rail and Rapid Transit* **233** (2) 160-169

[4] Ji Y J and Ren L H 2018 Anti-overturning capacity and critical roll angle of straddling monorail vehicle *Proceedings of the Institution of Mechanical Engineers, Part F: Journal of Rail and Rapid Transit* **232** (23) 4420-4429

[5] Zhu E Y, Wang H L and Wang L 2019 New adjustment method for the width of monorail beams on curve *KSCE Journal of Civil Engineering* **23** (5) 2204-2214

[6] Jiang Y Z, Wu P B and Zeng J 2019 Comparison of the curve negotiation properties of two different articulated monorail vehicles *Proceedings of the Institution of Mechanical Engineers, Part F: Journal of Rail and Rapid Transit* **233** (8) 831-843

[7] Jiang Y Z, Wu P B and Zeng J 2020 Multi-parameter and multi-objective optimization of articulated monorail vehicle system dynamics using genetic algorithm *Vehicle System Dynamics* **58** (1) 74-91

[8] Bao Y L, Li Y L and Ding J J 2016 A case study of dynamic response analysis and safety assessment for a suspended monorail system *International Journal of Environmental Research and Public Health* **13** (11) 1121-1138

[9] Ministry of Housing and Urban-Rural Development of the People's Republic of China 2018 *Standard for Metro Gauges* (Beijing: China Construction Industry Press)

[10] Ministry of Housing and Urban-Rural Development of the People's Republic of China 2008 *Code for Straddle Monorail Transit* (Beijing: China Construction Industry Press)